2015

Diachronic analysis of salt-Affected areas using remote sensing techniques: the case study of Biskra area, Algeria

Gabriela M. Afrasinei
Universita degli Studi di Cagliari

Maria T. Melis
Universita degli Studi di Cagliari

Cristina Buttau
Universita degli Studi di Cagliari

John M. Bradd
University of Wollongong, jbradd@uow.edu.au

Claudio Arras
Universita degli Studi di Cagliari

See next page for additional authors

Publication Details

Afrasinei, G. M., Melis, M. T., Buttau, C., Bradd, J. M., Arras, C. & Ghiglieri, G. (2015). Diachronic analysis of salt-Affected areas using remote sensing techniques: the case study of Biskra area, Algeria. Proceedings of SPIE, Vol. 9644: Earth Resources and Environmental Remote Sensing/GIS Applications VI (pp. 96441D-1 - 96441D-15). United States: S P I E - International Society for Optical Engineering.

Diachronic analysis of salt-Affected areas using remote sensing techniques: the case study of Biskra area, Algeria

Abstract
In the Wadi Biskra arid and semi-arid area, sustainable development is limited by land degradation, such as secondary salinization of soils. As an important high quality date production region of Algeria, it needs continuous monitoring of desertification indicators, since the bio-physical setting defines it as highly exposed to climate-related risks. For this particular study, for which little ground truth data was possible to acquire, we set up an assessment of appropriate methods for the identification and change detection of salt-affected areas, involving image interpretation and processing techniques employing Landsat imagery. After a first phase consisting of a visual interpretation study of the land cover types, two automated classification approaches were proposed and applied for this specific study: decision tree classification and principal components analysis (PCA) of Knepper ratios. Five of the indices employed in the Decision Tree construction were set up within the current study, among which we propose a salinity index (SMI) for the extraction of highly saline areas. The results of the 1984 to 2014 diachronic analysis of salt - affected areas variation were supported by the interpreted land cover map for accuracy estimation. Connecting the outputs with auxiliary bio-physical and socio-economic data, comprehensive results are discussed, which were indispensable for the understanding of land degradation dynamics and vulnerability to desertification. One aspect that emerged was the fact that the expansion of agricultural land in the last three decades may have led and continue to contribute to a secondary salinization of soils. This study is part of the WADIS-MAR Demonstration Project, funded by the European Commission through the Sustainable Water Integrated Management (SWIM) Program (www.wadismar.eu).

Disciplines
Medicine and Health Sciences | Social and Behavioral Sciences

Publication Details
Afrasinei, G. M., Melis, M. T., Buttau, C., Bradd, J. M., Arras, C. & Ghiglieri, G. (2015). Diachronic analysis of salt-Affected areas using remote sensing techniques: the case study of Biskra area, Algeria. Proceedings of SPIE, Vol. 9644: Earth Resources and Environmental Remote Sensing/GIS Applications VI (pp. 96441D-1 - 96441D-15). United States: S P I E - International Society for Optical Engineering.

Authors
Gabriela M. Afrasinei, Maria T. Melis, Cristina Buttau, John M. Bradd, Claudio Arras, and Giorgio Ghiglieri

Diachronic analysis of salt-affected areas using remote sensing techniques: the case study of Biskra area (Algeria)

Gabriela M. Afrasinei*[a], Maria T. Melis[a], Cristina Buttau[a], John M. Bradd[b], Claudio Arras[a,c], Giorgio Ghiglieri[a,c]

[a]Department of Chemical and Geological Sciences, Lab. TeleGis, University of Cagliari, Via Trentino 51-09127 Cagliari, Italy (ghiglieri@unica.it); [b]School of Earth and Environmental Sciences, University of Wollongong, Northfields Ave, Wollongong 2522, NSW, Australia (jbradd@uow.edu.au);[c]Desertification Research Center–NRD, University of Sassari, Viale Italia 39-07100 Sassari, Italy (nrd@uniss.it);

ABSTRACT

In the Wadi Biskra arid and semi – arid area, sustainable development is limited by land degradation, such as secondary salinization of soils. As an important high quality date production region of Algeria, it needs continuous monitoring of desertification indicators, since the bio – physical setting defines it as highly exposed to climate – related risks. For this particular study, for which little ground truth data was possible to acquire, we set up an assessment of appropriate methods for the identification and change detection of salt-affected areas, involving image interpretation and processing techniques employing Landsat imagery. After a first phase consisting of a visual interpretation study of the land cover types, two automated classification approaches were proposed and applied for this specific study: decision tree classification and principal components analysis (PCA) of Knepper ratios. Five of the indices employed in the Decision Tree construction were set up within the current study, among which we propose a salinity index (SMI) for the extraction of highly saline areas. The results of the 1984 to 2014 diachronic analysis of salt – affected areas variation were supported by the interpreted land cover map for accuracy estimation. Connecting the outputs with auxiliary bio-physical and socio-economic data, comprehensive results are discussed, which were indispensable for the understanding of land degradation dynamics and vulnerability to desertification. One aspect that emerged was the fact that the expansion of agricultural land in the last three decades may have led and continue to contribute to a secondary salinization of soils. This study is part of the WADIS-MAR Demonstration Project, funded by the European Commission through the Sustainable Water Integrated Management (SWIM) Program (www.wadismar.eu).

Keywords: arid areas, land degradation, desertification, salinization, land cover, decision tree, principal component analysis, Knepper ratios, Landsat, change detection

1. INTRODUCTION

In this paper we focus on the Biskra study area in Algeria, characterised by an arid and semi-arid climate, where sustainable development requires the monitoring of land degradation processes as it withstands the understanding of desertification dynamics. The current study concentrates on the assessment of the dynamics of desertification and land degradation phenomena and proposes an adaptive methodology incorporating remote sensing techniques and ancillary data for the estimation of quantitative and qualitative change of degradation – indicating features such as soil salinization. This study is also part of the WADIS-MAR Demonstration Project, funded by the European Commission through the Sustainable Water Integrated Management (SWIM) Programme (www.wadismar.eu). The project aims at the promotion of an integrated, sustainable water harvesting and agriculture management in two watersheds in Tunisia and Algeria.

Out of the various forms of land degradation, soil salinization is the main menace for sustainable agriculture [1]. It is estimated that more than half of the irrigated land in arid and semiarid regions of the world is affected to some degree by salinization and that millions of hectares of agricultural land have been abandoned because of salinity build-up [1-3]. In these areas, leached salts concentrate in slow – flowing groundwater and are brought to the soil surface through high evapotranspiration and inappropriate agricultural activities intensify these processes [1], as in the case of the Biskra area. Remote sensing has been proven to be a useful tool for multi-temporal analysis through detection and evaluation of desertification indicating features for decision support, among other usages [4, 5]. Problems regarding image

*gma343@uowmail.edu.au; phone +39 070 6757701

classification of several features in these particular areas have been reported by the scientific community, either with supervised, unsupervised classifications or spectral mixture methods. These issues mainly regard spectral confusion of salt features with other land ones, especially urban fabric, bare land or carbonate-rich ones [1, 3, 6, 7].
Soil salinity mapping through remote sensing is translated through spectral characterization of the contained abundant salt minerals. Knepper (1989) proposed specific band ratios for the delineation of hydroxyl – bearing minerals, hydrated sulphates and carbonates, vegetation and iron oxides and hydroxides, namely the 5/7:3/1:3/4 red-green-blue (RGB) combination, used mainly for geological remote sensing mapping [8], but the novelty of the current study is that it is employed for salt features identification. Thus, two different classification schemes are proposed in this study: 1) a decision tree analysis (DTA) [9] [10, 11], [3] based on spectral analysis, band transformation and expert-knowledge and 2) the analysis of the Principal Components (PCA) of Knepper ratios, adequate in the fast, spectral-based delineation of mineral components. In the Biskra area, ground truth data was difficult to achieve in the correct amount needed for such studies, thus available ancillary data were used as basis throughout the study phases. The methodology proposed in this study arises from the need to tackle with two types of problems: 1) the environmental issue present in the area of study, hence soil salinity and secondary salinization and 2) from the methodical point of view, hence the limited or no access to field data or to undergo field survey oneself and the spectral confusion of very reflective desert features. Firstly, the visual interpretation of one Landsat scene of 2011 was done, sustained by a large set of ancillary data. In the second phase, the decision tree was built based on spectral analysis and existing indices assessment and nonetheless, the proposing new ones according to purpose. Thirdly, the PCA was applied to Knepper ratios composite, as a support for the decision tree classes' verification. The accuracy estimation of the decision tree results for the 2011 scene was done using the previously interpreted land cover map and the IsoDATA classified PCA images. The final objective of this paper is the use of remote sensing imagery in change detection, hence a consistent number of works have been reviewed for the current study that discuss or use satellite imagery [12-14] but the results show a discrepancy in the accuracy assessment and the degree of the replicability of algorithms or methods applied [15].We try to minimise these issues proposing the methodology and methods described in the following sections.

2. STUDY SITE

The first study site, illustrated in figure 1, is located in North-East sector of the Northern Sahara and covers an area of about 500 000 hectares. It mostly overlays the Wilaya of Biskra and to a smaller extent the one of Batna. It represent mainly a piedmont area, passing from the Aures mountainous and hilly domain in the North to the Sahara plain in the South, with fine-clayey deposits and vast alluvial fans and small mountain ranges in the middle - slope area.

The area can be divided in two zones: the *Occidental Zab* and the *Oriental* one (as shown in figure 1), where Oued Biskra constitutes the limit between the two zones. Locally known as the *Zibans palmeraie* (palm grove) or the *Occidental Zab*, the irrigated area exceeds 65 000 ha and draws more than 600 million of m^3 per year, with the Tolga area as international exporter of high – quality dates (*Deglet Nour*). The importance of these palm groves is due mostly to the presence of very productive and shallow aquifers highly exploited for more than one century [16], with an average salinity from 2 to 4 g/l, hence the increase of surface salinity and gypsum encrustment. The land use mainly regards date palm plantations and extended greenhouse cultivations (vegetable cultivations), followed by open field cultivations.

To the East, the *Oriental Zab* domain of the *Zibans* area, the landscape is characterised by vast alluvial fans and a plain modelled by *wadi* courses, with their source area in the Atlas and eventually fading into the great depression of the greater watershed of Chott Melrhir, reaching an average of – 80 m below sea level. Open field and industrial cultures have become an intense practice in the last decades, as these ones, unlike phoeniciculture, do not require a shallow aquifer [17], but usage of deep groundwater has increased in the last decades.

From the geological point of view, the Biskra area is located within the transition zone between the folded Atlas domain in the Northern part of the area and the desert and flat domain of Sahara, in the South. The area is characterized by the superposition of several folding events occurring from Middle Eocene to Pleistocene that strongly influence the geometry of the main aquifers [18, 19]. The lithological stratigraphy is composed mainly out of clay and sand alternations (Quaternary and Mio-Pliocene), gypsum clays and evaporitic deposits (middle Eocene), limestone (Lower Eocene), limestone, gypsum clays and halite (Senonian), dolomitic limestone and dolomites (Turonian) and clay, marlstone and gypsum belonging to Cenomanian.

The climate is hot and dry, stretching over the semi-arid, arid and pre-desert zones, with an annual mean of 21°C. The maximum frequency of rainfalls is in November and March and the average annual total received rainfall is about 200 mm but the annual mean rainfall is less than 30 mm. The minimum rainfall is almost null in the months of July and August.

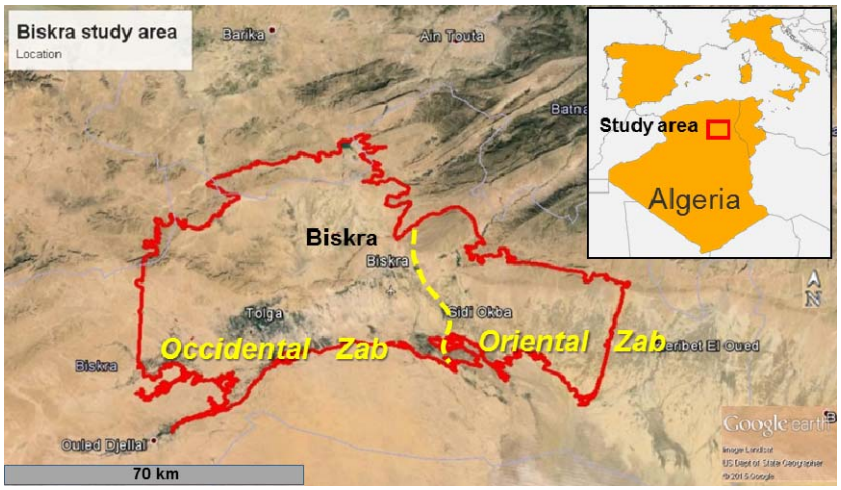

Figure 1. Study area

3. MATERIALS AND DATA

A large set of ancillary data was used for the visual interpretation phase of the land cover and land use classes (LCLU), comprising available spatial data, geological and topographical maps, agricultural calendars, statistics and pedological reports, mainly provided by local entities and institutions such as *L'Agence Nationale des Ressources Hydrauliques*, Algeria, (ANRH), Institut Technique de Développement de l'Agronomie Saharienne (ITDAS) and other local entities. Available Google Earth high resolution satellite images and data were also consulted.

All Landsat images were obtained by the courtesy of the US Geological Survey (USGS, earthexplorer.usgs.gov) and they were chosen avoiding exceptional humid years, which were irrelevant for this study. Consulting climate data, the imagery at the beginning of the dry season and at the end of it was the most suitable, but the choice of the scenes was restricted by cloud coverage. Images from 1984 to 2014 were chosen, as presented in table 1. ArcGIS 10.2 was employed for geospatial data consultation and geo-processing and ENVI 5.2 software (Exelis VIS, Boulder, CO) was used for the pre-treatment and processing of satellite data.

Since this study approaches an inter- and intra-annual change analysis, 2 images per each one of the four years were chosen: one at the beginning and one at the end of the dry season. This is because there is a maximum vegetation peak at the end of May, after the winter – spring rainfalls and a minimum vegetation peak at the end of the dry season, in August-September.

The years were chosen at an interval of about 10 years, starting with 1984, the oldest available. We have taken into account the fact that, in these particular areas, substantial changes in various types of land cover are due to the seasonal regime, especially soil salinization which is very sensitive to either excess or lack of water income. These were chosen after a careful consultation of climate data (Biskra weather station, tutiempo.org) in order to avoid pre or post heavy rainfall days, especially for the post dry season dates. The 2011 scene used for visual interpretation was not inserted in the multi-temporal analysis, being used only for accuracy assessment.

Table 1. Landsat scenes used for Biskra area

Satellite	WRS Path	WRS Row	Year Acquisition	Day of acquisition- Julian date	Date
LT5	194	36	1984	182	30 June
LT5	194	36	1984	246	2 Sept
LT5	194	36	1995	148	28 May
LT5	194	36	1995	228	16 Aug
LT5	194	36	2007	149	29 May
LT5	194	36	2007	229	17 Aug
LT5	194	36	2011	160	9 June
LC8	194	36	2015	123	3 May
LC8	194	36	2015	219	7 Aug

4. METHODS AND DATA PROCESSING

1.1. Visual interpretation

The visual interpretation of LCLU maps assisted as reference data due to its detail, quality (1: 70 000 scale, around 40 LCLU classes) and high expert knowledge validity [3]. The methodological and classification approach was adapted from various land cover programs implemented either in Europe, such as CORINE land cover or the African ones [20-23] which allowed us to define visual interpretation keys and variables and a land cover nomenclature and class description adapted to the local context. In the Biskra area, the interpretation of the Landsat TM5 of 9th of June 2011, path 194, row 36 resulted in 37 LCLU classes that were defined based on ancillary data, given that ground truth data was difficult to obtain. This step served for the overall acquaintance with the study area in terms of land cover and land use and for the specific purpose of this paper, only the saline areas class were taken into consideration for comparison to DTA and Knepper PCA results.

1.2. Processing and classification methods

The level L1T products were subset to study area extent, radiometrically calibrated to obtain top of atmosphere reflectance and Dark Object Subtraction (DOS) was applied for atmospheric correction, thus obtaining surface reflectance. Since the product employed ground control and relief models (as delivered by the provider, namely USGS), geometric correction was not performed [24] [25]. No topographic correction was applied as it has been reported by several authors as prone to over-correct values in plain areas and lose valuable information, especially in regions where spectral separability has such sensitive thresholds [26]. All images were verified for co-registration.

1.3. Spectral analysis for decision tree construction

This phase consisted of spectral information analysis using spectral enhancement techniques, horizontal and vertical spectral profiles analysis and 2D scatter plots investigation of salt features in order to understand their spectral behaviour in relation to features that can present similar spectral characteristics and confusion: carbonate-rich, clay-rich areas, bare land, urban fabric and outcropping rocks. For the spectral analysis, we have taken into consideration two factors: one is the maximum information content of the composite bands, as the larger the standard deviation is, the more the information content is derived from the composite bands; the other is the minimum affinity of the composite bands leading to significant independence and less redundant data. After reviewing several vegetation and salinity indices reported as successful in delineating salt-affected areas [5], the results that emerged were not completely satisfactory and observations were made in order to choose optimal band operations for decision tree integration. Consequently, band ratios and indices [5, 7] have been derived in order to discriminate as accurate as possible the features of interest, in order to support decision rules used for a decision tree classifier scheme. The decision tree analysis was chosen because

of its high flexibility of input data range and easiness of class extraction through multi-stage classification but at the same time because of its simplicity, being composed of "yes/no" decision nodes, which, according to a specified threshold, separates two classes from each node.

1.4. Knepper ratios and PCA

The principal components analysis was applied to Knepper composites of each year [8] in order to obtain a good spectral separability of land cover types and to evaluate its potential as approach of fast automated, user-independent classifier, as opposed to decision tree analysis that needs thorough computation for rules choice and threshold calculation. It is based only on the spectral information contained within the employed bands, but it does not allow other manipulation, which may be considered rigid, as it presents a consistent problem of mixed pixels. Thus, the obtained images present difficulty in applying a classifier and in order to avoid further errors, IsoDATA unsupervised classification was chosen, as it proved to be the most suitable, with maximum 50 iterations, a threshold of 2 % and 12 classes requested. The PCA analysis was applied for each one of the 9 assessed years.

5. RESULTS AND DISCUSSION

1.5. Decision tree analysis results

The indices and band math operations employed in the DTA is summarized in table 3. Finally, the decision tree map was obtained by applying vegetation, wetness, mineral and salinity indices as well as simple band ratios, mostly derived from the analysis of bands statistics, scatter plots and vertical and horizontal profiles of interest features but also from literature, as presented in figure 2 and table 2 [3, 5, 7, 24, 27-29]. The indices proposed for this study are constructed based on bands which present high spectral information covariance of the feature to be extracted. For example, in the case of *highly saline areas* class extraction, TM bands 1, 2 and 3 information are usually put together, in order to enhance the "brightness" features, divided by band 7, which presented the lowest reflectance values of salt features. Exponential or square root functions were used to force the emphasis of extreme values, helping in delineating high or moderate saline areas. The statistics of each index/math image were used in order to establish the thresholds for each decision node. The decision nodes and the resulting map are thus obtained, for each of the 8 dates. According to the lithological and vegetation cover of the area, the DT analysis and legend was adapted in order to classify the main land cover classes as well as classes of lithology distinguishable according to their spectral lithological response, which are described in table 3.

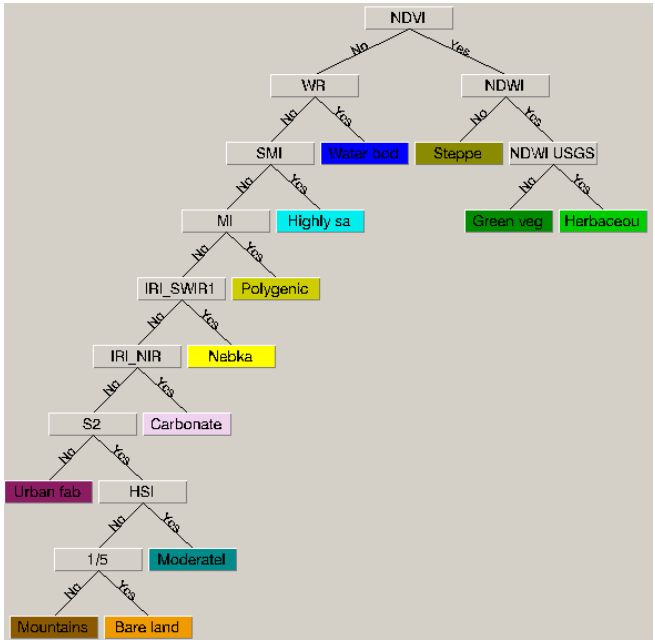

Figure 2. Decision tree binary decision nodes and resulting classes

Table 2. Indices analysed for decision tree construction, Biskra study area, Algeria (parent nodes only). Thresholds correspond to the indices applied for the 7 August 2015 image.

Parent nodes-decision	Expression	Band math (TM bands)	Indices	Reference
NDVI	b1 GE 0.24	(b4-b3)/(b4+b3)	Normalised Difference Vegetation Index	[5]
NDWI	b2 GE 0.01	(b4-b5)/(b4+b5)	Normalised Difference Water Index	[30]
NDWI USGS	b3 GE -0.39	(b3-b4)/(b3+b4)	Normalised Difference Water Index - USGS	[31], also known as Normalised Difference Salinity Index (NDSI) [32]
WR	b4 GE 1.0	b3/b4	Water Index	derived from [33]
SMI	b5 GE 0.74	sqrt(((b1^2)+(b2^2)+(b3^2))/b7)	Salt Minerals Index	proposed for this study
MI	b6 GE 0.028	(b1*b2*b3)/b4	Mineral Index	proposed for this study
IRI_SWIR1	b7 GE 0.88	sqrt(((b4^2)+(b7^2))/b5)	InfraRed Index – Short Wave InfraRed 1 (TM band 5)	proposed for this study
IRI_NIR	b8 GE 1.7	sqrt(((b5^2)+(b7^2))/(b4^2))	InfraRed Index – Near InfraRed (TM band 4)	proposed for this study
S2	b9 LE -0.32	(b1-b3)/(b1+b3)	Salinity Index 2	[5]
HSI	b10 GE 1.74	(b1+b2+b3)/b7	Hue Salinity Index	proposed for this study
1/5	b11 GE 0.22	b1/b5	Ratio 1/5	[27]

Table 3. Decision Tree class description

Green vegetation	Oasis vegetation, mainly palm groves, fruit trees plantation, types of small trees and tall shrubs rich in chrorophyll
Herbaceous vegetation	Annual crops, small natural herbaceous vegetation, small shrubs
Steppe	Typical dry shrub vegetation, woody correspondent to mountainous and piedmont areas
Urban fabric	Artificial, build-up surfaces, usually impervious
Nebka	Typical semi-arid aeolian coppice dunes, areas of sand plains (dunes) covered by sparse or no vegetation
Mountains/outcropping bedrock	Mountain ranges and slopes, scree, cliffs, including active erosion flats, outcropping bedrock
Carbonate-rich areas	Areas with a high carbonate component, limestone crust, outcropping limestone
Polygenic deposits	Deposits correspondent to alluvial fans, recent alluvial deposits, piedmont and glacis accumulations, with a strong clay, sand and coarse materials
Bare land	Land with no vegetation cover and of no land use
Highly saline areas	Areas rich in salt minerals components
Moderately saline areas	Areas that present moderate salinity
Water bodies	Water areas of natural or artificial origin

1.6. IsoDATA classification of Knepper ratios PCA

The results showed that the third principal component mostly contained salt minerals – related information. The first component, representing the highest covariance between the 3 ratio images, mostly contained important information on the sand component, and the second one, clay minerals, that mostly overlaid areas of alluvial fans, with loam and clayey components. The IsoData classification has presented difficulty in delineating the requested 12 main classes, some of which presenting similar characteristics to other existing ones, being unable to separate the *moderately saline areas* class. In order to allow comparison between the two sets of classification, the resulting DTA classification images to IsoDATA Knepper PCA classification images, the classes were evaluated for correspondence and the "improper" classes were not considered for analysis. In the figures 3 and 4, the classes which do not correspond to the expected resulting classes, are presented in white-grey-black levels and the class name denotes the fact that it is more likely to belong to that one. Thus, only *highly saline areas* class was considered and the other ones were merged into one class of *land*, for both DT and IsoData maps. Confusion matrix was applied for the error assessment and DTA images were set as "input files" and Knepper PCA images as "ground truth images". This analysis was applied for the 30 June 1984 pair of DT map and IsoData Knepper PCA map, the 9 June 2011 pair and 7 August 2015 pair, for both seasons. The first pair has given an overall accuracy of 70% but a kappa coefficient of 0.71; the third pair, on the other hand, has given an overall accuracy of 79.97% and a kappa coefficient of 0.58, as presented in table 4. This discrepancy may be related to the disadvantages of the IsoData classification method, its threshold set for class separation and number of iterations, as well as the different quality of satellite data, either in terms of noise or radiometric resolution. In fact, it must be mentioned that the 30 June 1984 image was more laborious for the construction of the DT and its node thresholds very different from the rest of the images, whilst the other 7 images have maintained very close threshold values of correspondent indices.

Table 4. Comparison and accuracy assessment of DTA according to LC map and IsoDATA of Knepper PCA map

	1984_182	2011_160	2011_160	2015_219
Classification methods pairing	DT_IsoData & Knepper_PCA	DT_IsoData & Knepper_PCA	DT & LC visual interpretation	DT_IsoData & Knepper_PCA
Employed classes	*highly saline areas*	*highly saline areas*	*highly saline areas*	*highly saline areas*
Kappa coefficient	0.71	0.57	0.41	0.58
Overall accuracy	70.30%	77.91	72.71%	79.97%

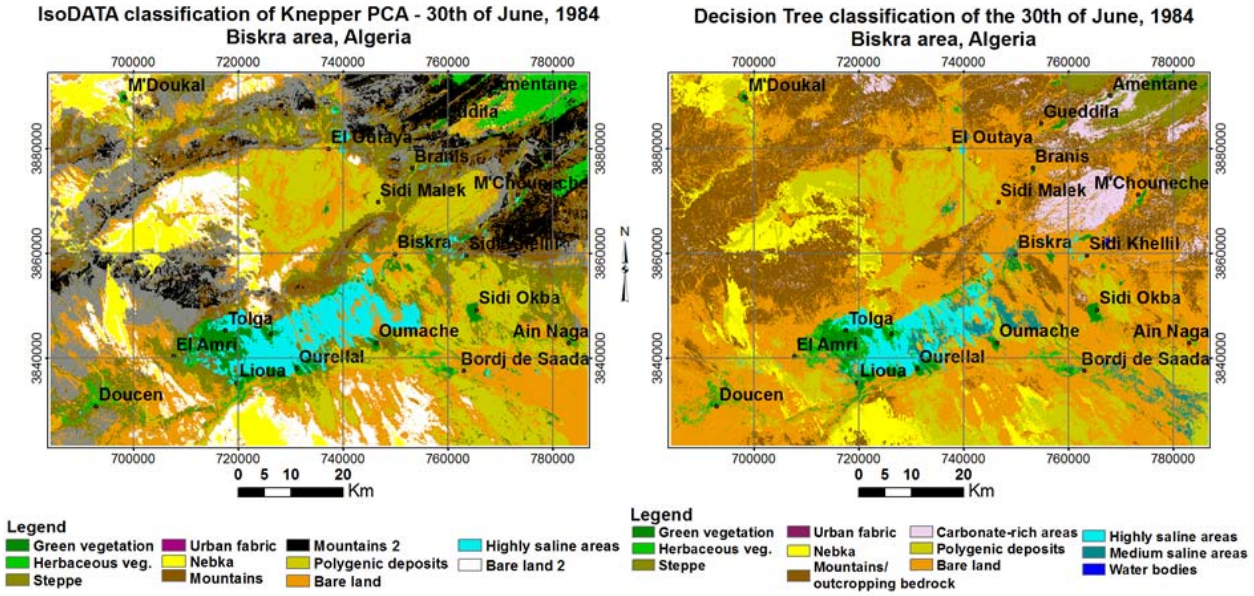

Figure 3. IsoDATA classification applied to Knepper ratios PCA and DTA classification of 30 June 1984 image

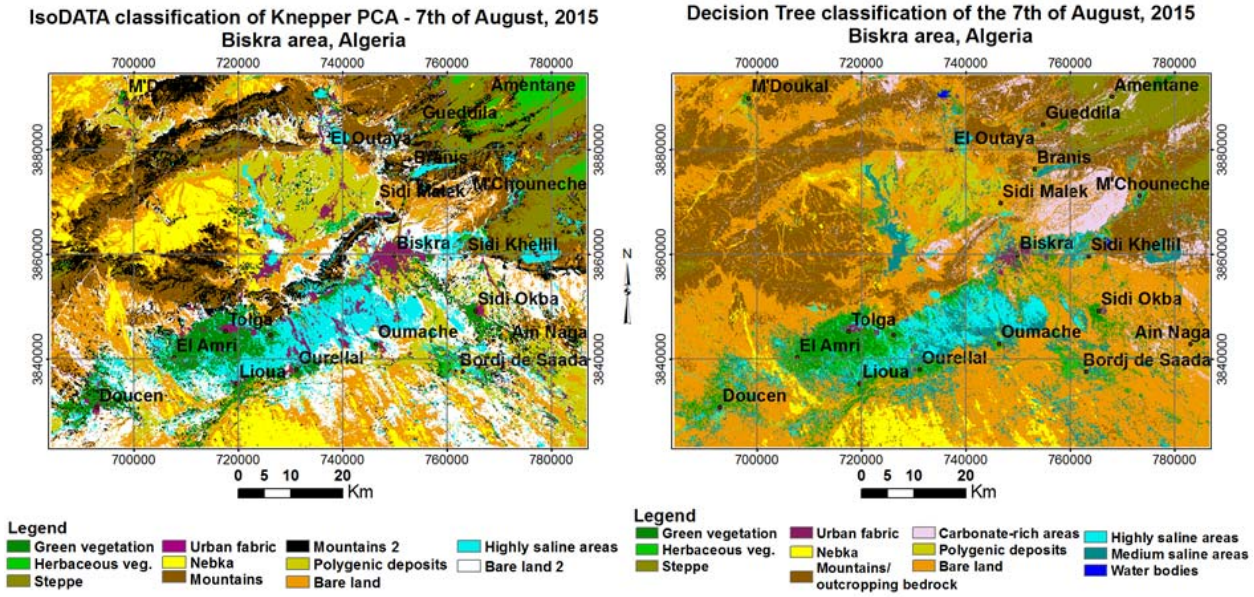

Figure 4. IsoDATA classification applied to Knepper ratios PCA and DTA classification of 7 August 2015 image

An important aspect to be emphasized is the fact that the decision tree offered more flexibility, as a multistage classifier, thus managing to delineate classes with higher control. The amount, complexity and types of spectral information put together in this single classifier makes it highly controllable, as opposed to other classification flows. The comparison to the visually interpreted land cover map was undergone through visual inspection for all classes, but for a quantitative assessment, the DTA map of 2011 was reduced to only two classes: "land" and "highly saline areas" and compared with the "saline areas" class of the LCLU map. Error matrix showed a matching of 72%, that can be due to the subjectivity of the user, since visual interpretation implies a series of variables taken into consideration by the user when delineating features (contours, hue, size, texture, location), but cannot allow the delineation of moderately saline areas. This class has a particular spectral response, not discriminative enough through visual interpretation, but only through spectral information extraction, i.e. an adequate index.

6. DISCUSSION

1.7. Change detection analysis

As a result of the DTA classification, we obtained the salinity/land cover maps for the chosen dates, as presented in figure 5. We approached change detection analysis in two ways: we have compared the images of each of the two analysed seasons from 1984 to 2015, but we have also looked at changes between one season and another, within a year. The changes of each class surface, expressed in percentages, for each date can be observed in figure 9, and the maps are presented in figures 5 to 8. For the easiness of the interpretation discussion, we will refer to the May-June images as belonging to the "wet season" and to the August-September images as "dry season".

From the intra-annual point of view, in all years, changes that occur between the end of the wet season and the end of the dry season, maintain similar pattern of change. More specifically, classes that are interchangeable remain as follows: *highly saline areas* have the most frequent interchange with *moderately saline areas*, *polygenic deposits* and *herbaceous vegetation* classes (decreasing in 1995, by 1.53% and in 2015 by 1.69% and increasing in 2007 by 17.63%); moderately saline areas mostly interchange with *highly saline areas*, *urban fabric*, *bare land* and *herbaceous vegetation* (with an increase of 60% in 1984, 100% in 1995, 93% in 2007 and 106% in 2015.

As an example of intra-annual change, the results of the detection analysis of 30 June and 2 September images of the year 1984, show that the *highly saline areas* class has decreased by 26%, mainly in the favour of *urban fabric* class, by 18.7%, *polygenic deposits* by 4.2% and *herbaceous vegetation*, by 2.1%, gaining only 1.4% and 1.9% of *water bodies* and *herbaceous vegetation* classes, respectively. The total changes, with gains and losses, represent -19.8%.

It must be mentioned that throughout the classification process, both in DTA and Knepper PCA, there has been a strong spectral confusion of "highly saline areas" class and the "water bodies" one (consisting of one lake in the hole image in 1984 and 1995, after which another one is visible after 2007, in the northern part of the areas, which is reported to be due to the construction of a dam). This confusion problem has been solved only throughout the DTA, using the ratio Red/Infrared (presented as WR in table 2). The urban fabric are expected to be classified under saline areas as it has been noticed to have similar spectral behaviour to these latter ones in all the analysed images. Thus, the changes regarding saline areas-urban fabric may not be a true change, but a misclassification due to this spectral confusion. In the year 1984, the *moderately saline areas* have an overall increase of 60%, mainly in the disfavour of urban fabric, water bodies and herbaceous vegetation.

The fact that there is a constant interchange between either highly saline areas and *herbaceous vegetation* classes or between *moderately saline area* and *herbaceous vegetation*, gives way to the scenario that agricultural practices have the tendency to intensify the salinization processes, as the *herbaceous vegetation* class delineated in all images correspond more than 80% to agricultural areas, parcels of cultivated land, mostly recognizable by their rectangular shape, that may or not present chlorophyll response, but in some images denote the presence of humidity or re-worked land hues. These are found mainly in the Occidental Zab, in south-western part of the study area, in the Doucen area, around the Tolga Oasis, especially in the western part of it, known as El Amri and in Oriental Zab, the extended agricultural area between Sidi Okba and Ain Naga, as in can be observed in figure 5.

Concerning the inter annual changes analysis, the main trends observed from the change detection statistics are that *herbaceous vegetation* class presents a major increase (of 34%) in the disfavour of *green vegetation* class when comparing the 1984 and 2015 images dated at the beginning of the dry season, as opposed to a major increase of the *green vegetation* class in the disfavour of *herbaceous vegetation* class at the end of the dry season, of the same pair of years.

This comes as a natural change as the *herbaceous vegetation* class tends to be more sensitive to lack of rainfall and high temperature, as opposed to *green vegetation* class which is mainly composed of aridity-resistive palm groves, fruit trees and shrub vegetation.

Change detection results applied to the 1984 and 2015 pair (table 5 shows the dry season results) show that, in both seasons, the main classes with which *highly saline areas* class has interchanged are the urban fabric, moderately saline areas, herbaceous and green vegetation classes. It must be mentioned that both the *highly saline areas* and *moderately saline areas* classes have a major increase in the dry season (of 52 and 239%, respectively) compared to the wet season (of 24 and 164%, respectively).

Table 5. Example of change detection statistics: 2 September 1984 and 7 August 2015 change analysis

%	Moderately saline	Mountains	Carbonate-rich	Nebka	Polygenic deposits	Highly saline	Water	Steppe	Green veg.	Herb. Veg.	Urban	Bare land	Class Total
Unclassified	**0**	0	0	0	0	**0**	0	0	0	0	0	0	0
Moderately saline	**45.926**	2.83	0.318	1.694	9.867	**25.672**	5.91	0.489	4.963	19.417	25.749	16.984	100
Mountains	**0.124**	45.897	41.325	16.966	1.399	**0.002**	1.195	53.746	0.369	0.711	1.319	1.211	100
Carbonate-rich	**0.054**	2.557	47.795	0.065	0.573	**0.024**	0.598	6.091	0.068	0.141	1.572	0.545	100
Nebka	**0.147**	2.435	0.01	52.096	11.436	**0.06**	0.133	0.02	0.125	0.696	0.013	5.922	100
Polygenic deposits	**3.784**	0.891	0.214	0.928	26.554	**4.198**	0	0.073	0.314	2.238	2.797	5.35	100
Highly saline	**28.178**	**0.416**	**0.051**	**0.391**	**3.52**	**46.708**	**5.511**	**0.031**	**1.068**	**6.985**	**5.755**	**2.974**	**100**
Water	**0.098**	0.037	0.008	0	0.031	**0.001**	76.029	0.005	0.009	0.028	0.453	0.043	100
Steppe	**0.955**	0.852	1.338	0.395	1.378	**0.528**	4.515	35.354	15.035	7.404	4.036	1.477	100
Green veg.	**3.339**	0.58	0.094	0.37	0.751	**8.585**	0.93	0.72	46.935	17.569	1.652	1.714	100
Herb. Veg.	**4.772**	0.6	0.138	0.616	1.397	**9.33**	2.523	0.501	18.558	16.835	3.011	2.399	100
Urban	**1.458**	0.094	0.085	0.012	0.173	**3.116**	0.531	0.094	2.143	2.883	38.617	0.696	100
Bare land	**11.166**	42.81	8.624	26.468	42.921	**1.775**	2.125	2.876	10.412	25.092	15.026	60.684	100
Class Total	**100**	100	100	100	100	**100**	100	100	100	100	100	100	0
Class Changes	**54.074**	54.103	52.205	47.904	73.446	**53.292**	23.971	64.646	53.065	83.165	61.383	39.316	0
Image Difference	**239.001**	-35.444	-10.7	7.961	-31.962	**52.909**	154.316	-46.29	16.819	0.362	442.654	37.919	0

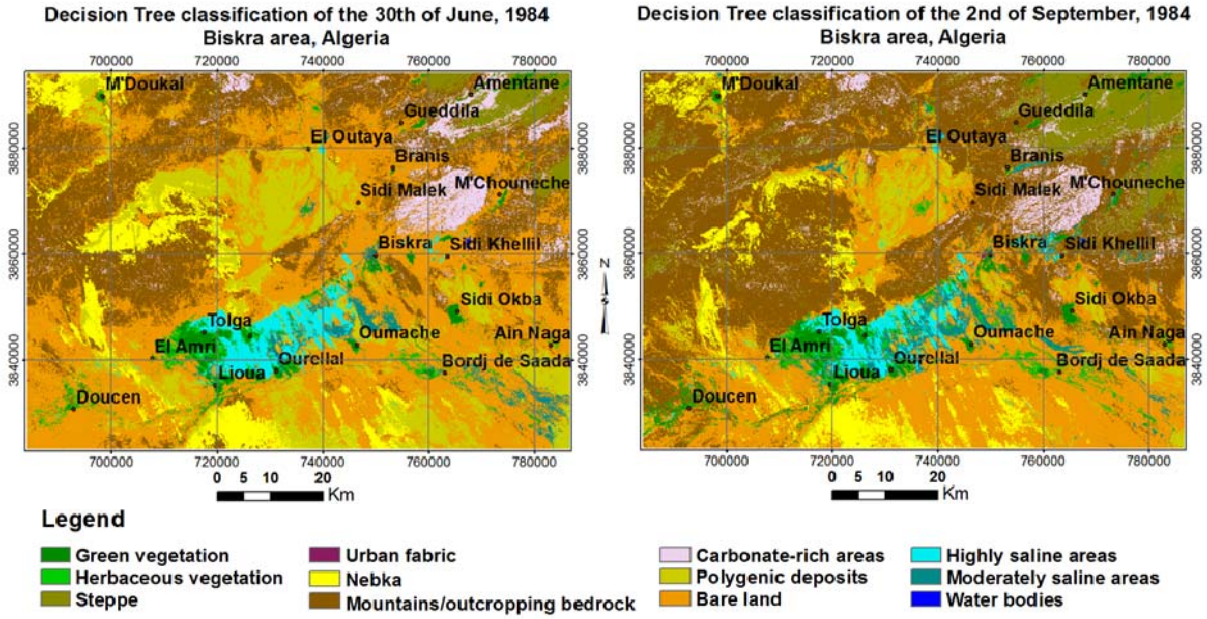

Figure 5. Decision Tree classification applied to 1984 images

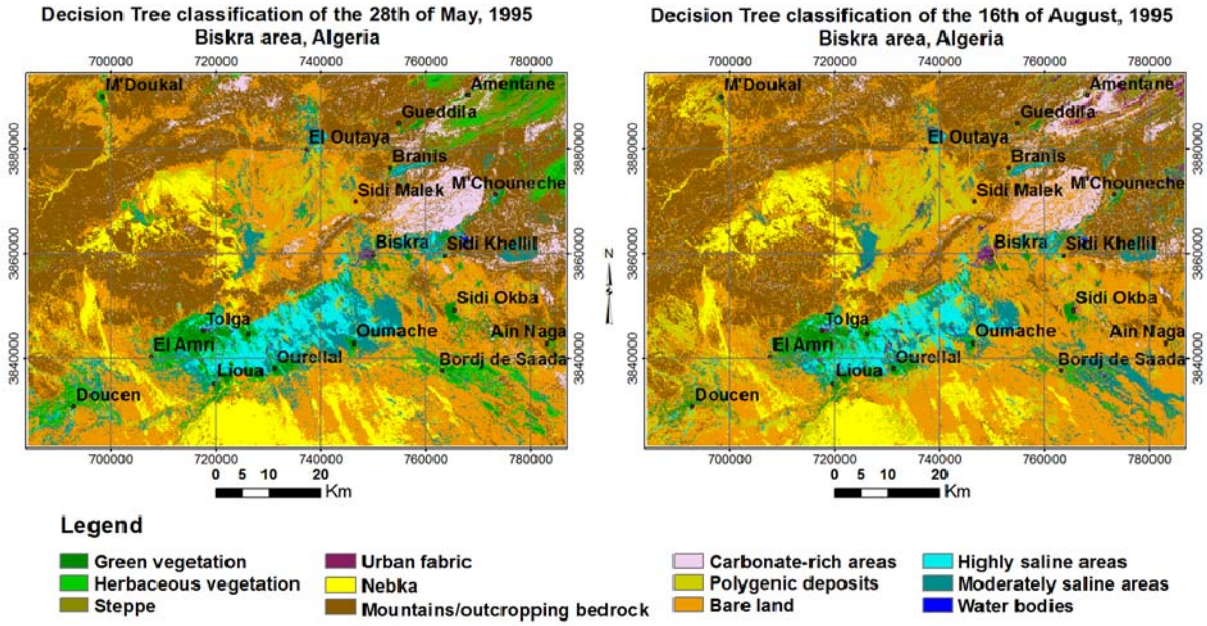

Figure 6. Decision Tree classification applied to 1995 images

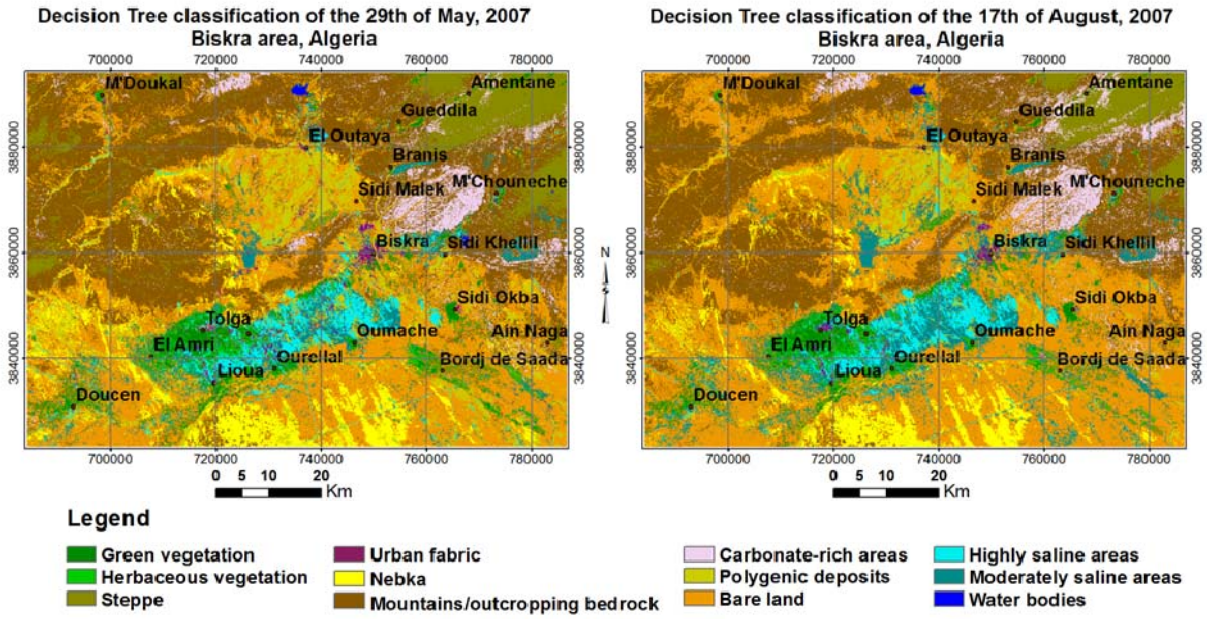

Figure 7. Decision Tree classification applied to 2007 images

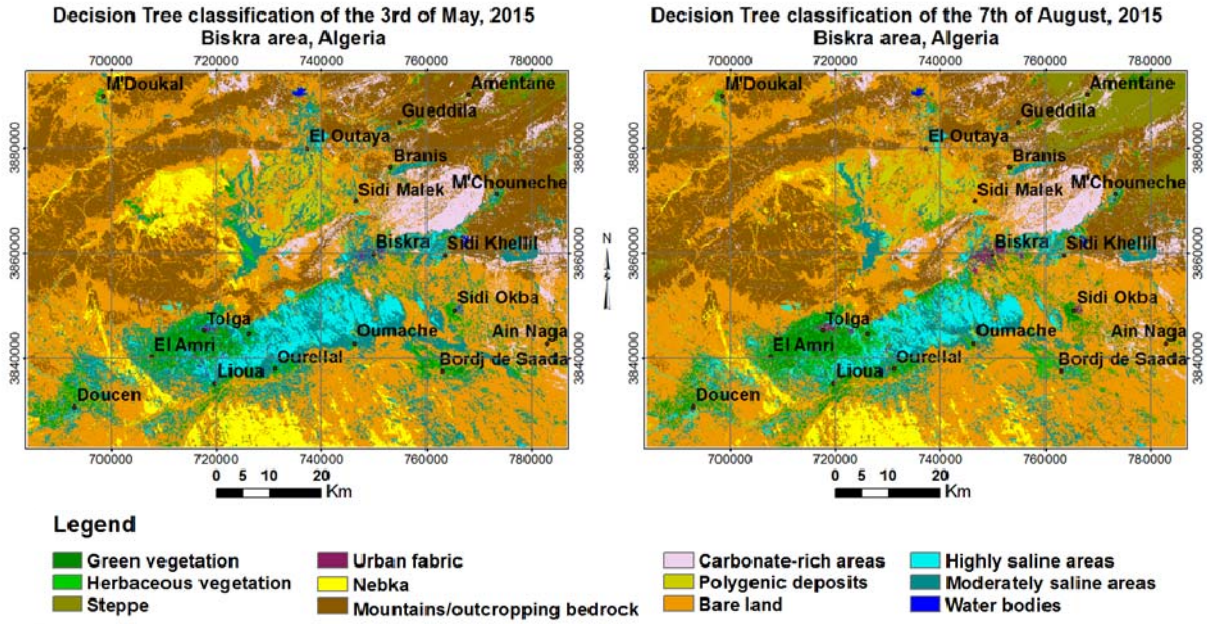

Figure 8. Decision Tree classification applied to 2015 images

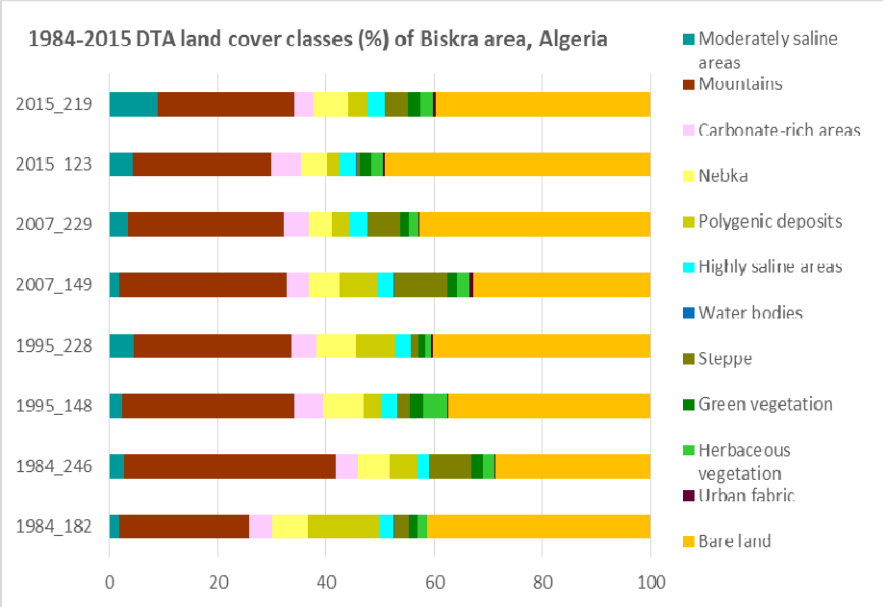

Figure 9. Class coverage statistics for each analysed date (percentage)

1.8. Saline areas mapping

In the Biskra area, the spectral analysis showed that the main factors affecting the reflectance of salt-affected soils are quantity and mineralogy of salts, together with soil moisture, colour, impurities content and surface roughness. The mineralogy of carbonate, sulphate and chloride salts determines the presence or absence of absorption features in the electromagnetic spectrum, associated with internal vibration modes due to excitation of overtones and combination tones of the fundamental anion groups (e.g. HOH, OH^-, CO_3^{2-}, SO_4^{2-}) [29, 34].

Regarding Biskra area, the issues encountered in the current study were those related to spectral confusion between saline areas, alluvial clayey material, carbonate – rich soils, and outcropping limestone. Applying solely salinization indices reported as having high accuracy when mapping salinity in similar areas [5, 32, 35], results were not satisfactory, since clay and silt-rich soils, urban fabric features, bare land and carbonate-rich surfaces were identified together with saline areas. The application of both decision tree and PCA of Knepper ratios showed satisfactory results but an overall accuracy of around 76,06 % which may be due to the user-dependency of the two datasets (DTA, LCLU map) of the total of three employed (the aforementioned and Knepper PCA).

However, the results confirm that surface features common in drylands, such as braided stream beds, eroded terrain surfaces with truncated soils, and non-saline silt-rich structural crusts, can generate high levels of reflectance, similar to those of areas with high salt concentration, as stated by [29].

7. CONCLUSIONS

The employment of the Decision Tree classifier has proven to be more flexible and adequate for the extraction of highly saline and moderately saline areas and major land cover types, as it allows multi-source information and higher user control. The results were compared to IsoDATA classification maps applied to Knepper ratios Principal Component Analysis and were proven to have a substantial advantage over this latter method. Five of the indices employed in the Decision Tree construction proposed for the current study have given satisfactory results. The accuracy of the salinity index (SMI) proposed in this paper for the extraction of highly saline areas was verified throughout 2 other mapping methods, being of around 76,06%. Applying post classification change detection (ENVI), the statistics for 1984 to 2014 analysis, comprising images acquired at the end of the wet season and at the end of the dry season, have shown an

overall increase of 53 % of the highly saline areas surface. The *moderately saline areas* class was noticed to have variations from one year to another, as it was considered to be very sensitive to seasonal conditions, but it presented an overall increase of over 100%. One of the important aspects that emerged from the diachronic series analyses is that the expansion of open field and industrial agriculture practices in the last three decades have led and continue to contribute to a secondary salinization of soils. In the Occidental Zab, the increase in salinized soils correspond to the expansion of phoeniciculture and market gardening (often greenhouse) but in the Oriental Zab, the large scale industrial agriculture, that required also a large number of deep wells (given the 200-300 m depth of the exploitable groundwater), has caused sporadic local appearance of small patches of salinized surfaces all along the lower slope of the alluvial fan area.

ACKNOWLEDGEMENTS

We wish to express our sincere appreciation to the TeleGIS Laboratory team of the University of Cagliari (Italy) and the WADIS-MAR team for the possibility of conducting the current research. We also wish to thank the Algerian WADIS-MAR partners, *Institut Technique de Développement de l'Agronomie Saharienne*, Biskra, Algeria (ITDAS) and *Agence Nationale des Ressources Hydrauliques*, Algeria (ANRH) for the provided data and collaboration. We wish to acknowledge also to the Spatial Analysis Laboratory of the University of Wollongong, Australia for the invaluable support provided during the undertaken research internship and their collaboration.

REFERENCES

[1] M. H. Fares, and C. G. Philip, [Characterization of Salt-Crust Build-Up and Soil Salinization in the United Arab Emirates by Means of Field and Remote Sensing Techniques] CRC Press, (2008).

[2] A. A. Masoud, and K. Koike, “Arid land salinization detected by remotely-sensed landcover changes: A case study in the Siwa region, NW Egypt,” Journal of Arid Environments, 66(1), 151-167 (2006).

[3] A. A. Elnaggar, and J. S. Noller, “Application of Remote-sensing Data and Decision-Tree Analysis to Mapping Salt-Affected Soils over Large Areas,” Remote Sensing, 2(1), 151-165 (2010).

[4] A. Abbas, S. Khan, N. Hussain *et al.*, “Characterizing soil salinity in irrigated agriculture using a remote sensing approach,” Physics and Chemistry of the Earth, 55-57(0), 43-52 (2013).

[5] A. Allbed, and L. Kumar, “Soil Salinity Mapping and Monitoring in Arid and Semi-Arid Regions Using Remote Sensing Technology: A Review,” Advances in Remote Sensing, 02(04), 373-385 (2013).

[6] J. Farifteh, F. van der Meer, M. van der Meijde *et al.*, “Spectral characteristics of salt-affected soils: A laboratory experiment,” Geoderma, 145(3–4), 196-206 (2008).

[7] N. M. Khan, V. V. Rastoskuev, E. V.Shalina *et al.*, [Mapping Salt-affected Soils Using Remote Sensing Indicators - A Simple Approach With the Use of GIS IDRISI -], (2001).

[8] R. L. Langford, “Temporal merging of remote sensing data to enhance spectral regolith, lithological and alteration patterns for regional mineral exploration,” Ore Geology Reviews, 68(0), 14-29 (2015).

[9] P. Rao, S. Chen, and K. Sun, "Improved classification of soil salinity by decision tree on remotely sensed images." 6027, 60273K-60273K-8.

[10] C. H. Matthew, [Classification Trees and Mixed Pixel Training Data] CRC Press, (2012).

[11] P. K. Srimani, and S. N. Prasad, “Decision tree classification model for land use and land cover mapping- a case study” International Journal of Current Research, (2012).

[12] H. Fu, L. Gu, R. Ren *et al.*, "Land salinization classification method using Landsat TM in western Jilin Province of China." 9220, 92200U-92200U-12.

[13] Q. Kang, R. Yu, Z. Zhang *et al.*, "Remote sensing application of soil salinization based on multi-source images." 6045, 60452V-60452V-7.

[14] M. Bouaziz, R. Gloaguen, and B. Samir, "Remote mapping of susceptible areas to soil salinity, based on hyperspectral data and geochemical, in the southern part of Tunisia." 8174, 81740Z-81740Z-7.

[15] F. Nutini, M. Boschetti, P. A. Brivio *et al.*, “Land-use and land-cover change detection in a semi-arid area of Niger using multi-temporal analysis of Landsat images,” International Journal of Remote Sensing, 34(13), 4769-4790 (2013).

[16] G. Ghiglieri, M. O. B. Sy, H. Yahyaoui *et al.*, "Design of artificial aquifer recharge systems in dry regions of Maghreb (North Africa)." FlowPath2014 - National meeting on nydrogeology - Abstract book.
[17] A. Bougherara, and B. Lacaze, [Etude preliminaire des images Landsat et Alsat pour le suivi des mutations agraires des Ziban (extrême nord-est du Sahara algérien) de 1973 à 2007] Journées d'Animation Scientifique (JAS09) de l'AUF Alger Journées d'Animation Scientifique (JAS09) de l'AUF Alger (2009).
[18] C. Buttau, A. Funedda, A. Carletti *et al.*, "Studio geologico strutturale per indagini idrogeologiche dell'area compresa tra le regioni di Batna e Biskra (NE Algeria)." Rend Online Soc Geol It, 29, 13-16 (2013).
[19] M. d. l. H. Algerienne, [Notice explicative de la Carte Hydrogeologique de Biskra au 1/200.000] Ministere de l'Hydraulique Algerienne MdH, Alger, Algeria(1980).
[20] ETC/LC, and E. E. Agency, [CORINE Land cover. Technical guide] ETC/LC, European Environment Agency, (1999).
[21] J. Feranec, and J. Otahel, [The 4th level CORINE land cover nomenclature for the PHARE countries] Institute of Geography, Slovak Academy of Sciences, Bratislava, Slovak Republic(2000).
[22] G. Jaffrain, and EEA, [CORINE land cover outside of Europe. Nomenclature adaptation to other bio-geographical regions] Universidad de Malaga, ETCSIA, Spain(2011).
[23] G. Büttner, G. Maucha, M. Bíró *et al.*, [National CORINE Land Cover mapping at scale 1:50.000 in Hungary] FÖMI Remote Sensing Centre, Budapest, Hungary(2000).
[24] M. Hamid Reza, and R. Majid Shadman, "Decision Tree Land Use/ Land Cover Change Detection of Khoram Abad City Using Landsat Imagery and Ancillary SRTM Data," Scholars Research Library(Annals of Biological Research), 4045-4053 (2012).
[25] X. Pons, L. Pesquer, J. Cristóbal *et al.*, "Automatic and improved radiometric correction of Landsat imagery using reference values from MODIS surface reflectance images," International Journal of Applied Earth Observation and Geoinformation, 33(0), 243-254 (2014).
[26] S. Vanonckelen, S. Lhermitte, and A. Van Rompaey, "The effect of atmospheric and topographic correction methods on land cover classification accuracy," International Journal of Applied Earth Observation and Geoinformation, 24(0), 9-21 (2013).
[27] M. T. Melis, G. Afrasinei, O. Belkheir *et al.*, [Caratterizzazione spettrale delle aree interessate da salinizzazione nel bacino del Oued Biskra in Algeria a supporto delle politiche di gestione dell'acqua nell'ambito del progetto WADIS-MAR] ASITA, Riva del Garda(2013).
[28] V. L. Mulder, S. de Bruin, J. Weyermann *et al.*, "Characterizing regional soil mineral composition using spectroscopy and geostatistics," Remote Sensing of Environment, 139, 415-429 (2013).
[29] G. Metternicht, and J. A. Zinck, [Spectral Behavior of Salt Types] CRC Press, (2008).
[30] http://www.seos-project.eu/modules/agriculture/agriculture-c01-s03.html, [Remote Sensing and GIS in Agriculture Vegetation Indices (NDVI, NDWI)], (2014).
[31] S. K. McFeeters, "The use of Normalized Difference Water Index (NDWI) in the delineation of open water features," International Journal of Remote Sensing, 17(7), 1425–1432 (1996).
[32] N. M. Khan, V. V. Rastoskuev, Y. Sato *et al.*, "Assessment of hydrosaline land degradation by using a simple approach of remote sensing indicators," Agricultural Water Management, 77(1-3), 96-109 (2005).
[33] F. D. van der Meer, H. M. A. van der Werff, F. J. A. van Ruitenbeek *et al.*, "Multi- and hyperspectral geologic remote sensing: A review," International Journal of Applied Earth Observation and Geoinformation, 14(1), 112-128 (2012).
[34] I. Szabolcs, [Salt Affected Soils] CRC Press, (1989).
[35] A. A. Masoud, "Predicting salt abundance in slightly saline soils from Landsat ETM+ imagery using Spectral Mixture Analysis and soil spectrometry," Geoderma, 217-218, 45-56 (2014).